Quench Performance and Field Quality of FNAL Twin-Aperture 11 T Nb_3Sn Dipole Model for LHC Upgrades

Stoyan Stoynev, Nikolai Andreev, Giorgio Apollinari, Bernhard Auchmann, Emanuela Barzi, Susana Izquierdo Bermudez, Rodger Bossert, Guram Chlachidze, Joseph DiMarco, Mikko Karppinen, Alfred Nobrega, Igor Novitski, Lucio Rossi, Frederic Savary, David Smekens, Thomas Strauss, Daniele Turrioni, Gueorgui V. Velev, and Alexander V. Zlobin

***Abstract*—A 2-m-long single-aperture dipole demonstrator and two 1-m-long single-aperture models based on Nb_3Sn superconductor have been built and tested at FNAL. The two 1-m-long collared coils were then assembled in a twin-aperture Nb_3Sn dipole demonstrator compatible with the LHC main dipole and tested in two thermal cycles. This paper summarizes the quench performance of the FNAL twin-aperture Nb_3Sn 11 T dipole in the temperature range of 1.9–4.5 K. The results of magnetic measurements for one of the two apertures are also presented. Test results are compared to the performance of coils in a single-aperture configuration. A summary of quench propagation studies in both apertures is given.**

***Index Terms*—Accelerator magnets, large hadron collider, superconducting coils, magnet design, magnetic measurements, quench performance.**

I. Introduction

FNAL and CERN carry out a joint R&D program with the goal of developing a 6-m long 11 T Nb_3Sn dipole suitable for installation in the LHC. Such a magnet will provide a necessary longitudinal space for additional collimators in the LHC. Development of the 11 T Nb_3Sn dipole for the LHC collimation system upgrade started in 2011 [1]. The recent R&D status and plans of the project were reported in [2].

At FNAL a 2 m long single-aperture dipole demonstrator and two 1 m long single-aperture models based on Nb_3Sn superconductor have been built and tested in 2012–2014. The two 1 m long collared coils were then assembled in a twin-aperture Nb_3Sn dipole model MBHDP01 and tested in 2015–2016 in two thermal cycles. The MBHDP01 quench performance in the first thermal cycle was reported and compared to single-aperture models in [3]. After training at 1.9 K, the bore field in the twin-aperture model reached 11.6 T. This is 97% of its design field of 12 T [4] and is within 1% of the field level reached in the single-aperture models showing that no additional degradation was introduced during coil re-assembly in a twin-aperture configuration. In June-July 2016 MBHDP01 was retested with the main goals to check its training memory, measure field quality and further investigate quench propagation between the two apertures. This paper summarizes the twin-aperture magnet quench performance in two thermal cycles, and reports and discusses the observed quench propagation effects and the magnetic measurements in one of its apertures.

Manuscript received September 2, 2016; accepted November 28, 2016. Date of publication December 7, 2016; date of current version December 28, 2016. This work is supported by the Fermi Research Alliance, LLC, under contract no. DE-AC02-07CH11359 with the U.S. Department of Energy and European Commission under FP7 project HiLumi LHC, GA no. 284404.

N. Andreev, G. Apollinari, E. Barzi, R. Bossert, G. Chlachidze, J. DiMarco, F. Nobrega, I. Novitski, S. Stoynev, T. Strauss, D. Turrioni, G. V. Velev, and A.V. Zlobin are with Fermi National Accelerator Laboratory, Batavia, IL 60510 USA (e-mail: andreev@fnal.gov; apollina@fnal.gov; barzi@fnal.gov; bossert@fnal.gov; guram@fnal.gov; dimarco@fnal.gov; nobrega@fnal.gov; novitski@fnal.gov; stoyan@fnal.gov; strauss@fnal.gov; turrioni@fnal.gov; velev@fnal.gov; zlobin@fnal.gov).

B. Auchmann, S. Izquierdo Bermudez, M. Karppinen, L. Rossi, F. Savary, and D. Smekens are with the European Organization for Nuclear Research, CERN CH-1211, Genève 23, Switzerland (e-mail: bernhard.auchmann@cern.ch; susana.izquierdo.bermudez@cern.ch; Mikko.Karppinen@cern.ch; Lucio.Rossi@cern.ch; Frederic.Savary@cern.ch; david.smekens@cern.ch).

Color versions of one or more of the figures in this paper are available online at http://ieeexplore.ieee.org.

Digital Object Identifier 10.1109/TASC.2016.2634524

II. Magnet Design and Construction

Design concepts of the 11 T Nb_3Sn dipole in single-aperture and twin-aperture configurations, developed at FNAL and at CERN, are described in [1], [5]. Fabrication and operational parameters in the two different configurations are compared in [3], [6] where manufacturing details of the twin-aperture magnet are also provided.

The twin-aperture magnet MBHDP01 consists of two collared coils inside a common iron yoke with coils 5 and 7 around one aperture and coils 9 and 10 around the other aperture. The former coils were previously tested in MBHSP02 and the latter coils in MBHSP03, both were single aperture models of 1 m length and 60 mm aperture. MBHSP02 and MBHSP03 used 0.7 mm diameter RRP150/169 and RRP108/127 strands, respectively, and a 40 strand Rutherford cable with 12 mm wide and 25 μm thick stainless steel core.

All four coils were instrumented with voltage taps for quench detection and characterization. Typical voltage tap locations in the coils and mechanical and electrical connections in the twin-aperture magnet are shown in Figs. 1 and 2, respectively. In addition, quench antenna provided coarse longitudinal and additional timing information about quench locations. It was installed in the radial gap between the anti-cryostat (a.k.a. "warm finger") and the coil. There were five quench antenna channels instrumented for coils 9 and 10 and three for coils 5 and 7.

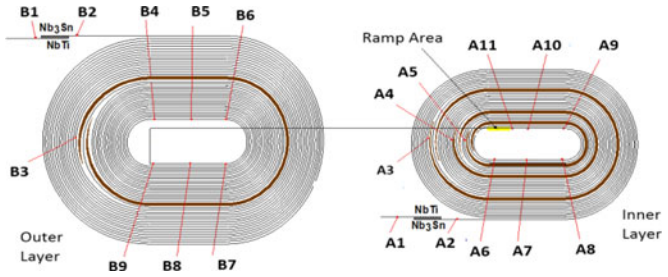

Fig. 1. Voltage tap scheme in a two-layer coil. External to the magnet splices between coils are also instrumented with voltage taps.

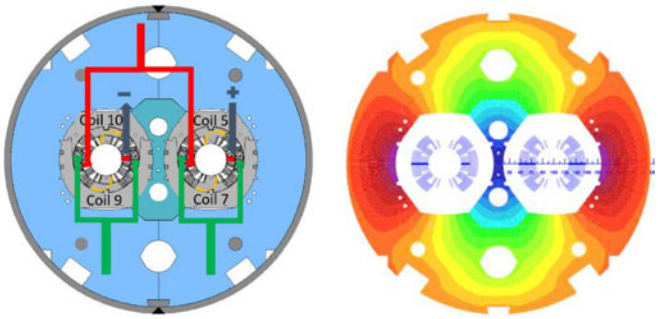

Fig. 2. Coil electrical connections (left) in the twin-aperture model and the field distribution diagram in the iron yoke (right). Coils are powered in series in the following order 5-7-9-10. Green lines (left) show the connections between coils in the same aperture whereas red lines show the connection between the two apertures; the three splices are realized outside the magnet.

III. Quench Performance

The twin-aperture dipole model MBHDP01 was tested at the FNAL Vertical Magnet Test Facility for the first time in February-March 2015, thermal cycle 1 (TC1). The cycle finished with three heater tests of up to 12 MIITs just after the last training quench. A limit of 18 MIITs was set to ensure the coil maximum temperature is well below 400 K [7], [8].

In June-July 2016 MBHDP01 was re-tested in thermal cycle 2 (TC2) with a new instrumentation header allowing for magnetic measurements in one of the two apertures. The "warm finger" was installed in the aperture with coils 9 and 10 to put the magnetic probe in the magnet bore. The TC2 consisted of an initial training run, magnetic and splice resistance measurements; second retraining run, heater tests, ramp rate studies; and a third retraining run, temperature dependence study, RRR measurements. Fig. 3 shows the quench current training and quench origins in TC2.

Fig. 4 summarizes the magnet bore field training in TC1 and TC2 calculated using the measured transfer function (TF) defined as the magnet bore field normalized to the magnet current. In TC1 magnet training started at relatively low field and was quite long. Therefore, the magnet was not fully trained. Coil 7 was limiting the magnet training with a few quenches in coil 10 in the semi-plateau region. Magnet training in TC2 started with the first quench field ~9% lower than the maximum bore field reached in TC1. Magnet re-training was also rather long. After 17 quenches the magnet quenched well below the maximum bore field reached in TC1. Coil 10 was responsible for the slow training in TC2, although each of the four coils quenched at least once, typically at the same locations as before around the second wedge in the inner layer.

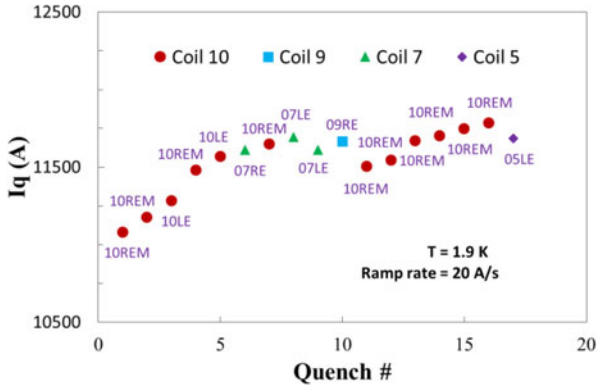

Fig. 3. MBHDP01 quench current training and quench origin in TC2. Quench antenna channels indicate the longitudinal quench location – lead end (LE), non-lead/return end (RE), middle position (M) or in between (LEM/REM).

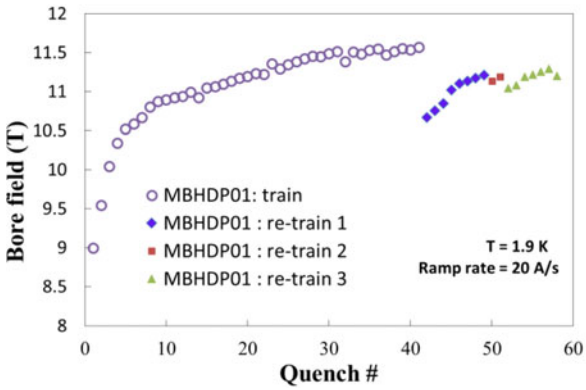

Fig. 4. MBHDP01 bore field training in TC1 and TC2 (retraining).

The data from the voltage taps and the quench antenna suggest that the quenches started close to the transition area between the coil straight section and the end regions. To mitigate possible influence of the "warm finger" on the coil cooling conditions, a second re-training run (Fig. 4) was performed with the "warm finger" sealed and evacuated. No improvement was observed and the test continued without sealing. The third training sequence after heater studies started again with a slightly reduced quench current. It was likely an effect from the heat depositions (with estimated <250 K maximal coil temperature) during the heater studies. The magnet never retrained to previous levels reached in TC1. Due to the slow progress, current gain of less than 40 A per quench, and a detraining quench in coil 5, the training in TC2 was stopped.

The temperature and ramp rate dependences, measured in TC1 and TC2, are shown in Figs. 5 and 6. Fig. 5 shows that there is no quench performance degradation at $T > 3$ K. However, at lower temperatures the quench currents are slightly lower than in TC1 as both Figs. 4 and 5 demonstrate. This deviation is likely due to the heat flux from the "warm finger" which may significantly affect the helium temperatures in the gap between the coil and "warm finger". It is consistent with the fact that all quenches in that test in TC2 developed in coil 10 whereas the corresponding quenches in TC1 developed in coil 7. It should be also emphasized that the effect of heat flux from the "warm finger" was amplified by the presence of the quench antenna boards installed on a plastic cylinder in the 10 mm radial gap between the coil and the "warm finger" wall. The obstructed

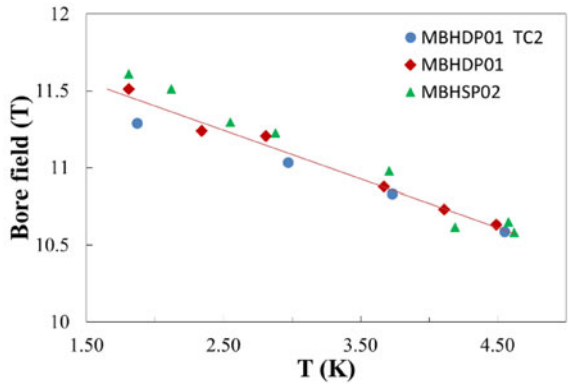

Fig. 5. Temperature dependence of the magnet bore field.

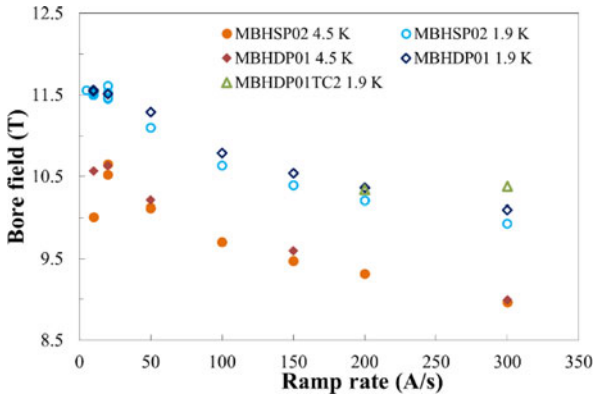

Fig. 6. Ramp rate dependence of the magnet bore field.

path for helium flow together with the heat load from the "warm finger" are possible explanation for the observations. Nevertheless few training quenches observed in the other aperture may indicate actual detraining of the magnet.

At the ramp rate of 300 A/s a higher quench current in TC2 was observed (see Fig. 6). This quench preceded the 200 A/s quench. It is likely due to a temperature fluctuation. Apart from this deviation, the behavior in the two apertures and between the two thermal cycles is similar.

Magnet training curves were parametrized using the first and maximum quench currents normalized to the short sample limit (SSL), number of quenches to reach certain level of training (in per cent of SSL), and current differentials. While the data are still being analyzed, Fig. 7 represents the current differential distributions for single and twin-aperture models. The spread, in particular at negative values, signals the more erratic training behavior in MBHSP02 and MBHSP03. The retraining of the coils in MBHDP01 was slower and very similar between TC1 and TC2 as indicated by peak positions.

In TC2 extensive splice resistance measurements were performed. All measurements pointed to an acceptable level of resistances, although NbTi/NbTi splices (between coils, outside the magnet) showed consistently higher resistance –1.0–1.5 nΩ compared to less than 0.4 nΩ for the rest.

IV. Quench Propagation

At the end of TC1, quench propagation between the two apertures was observed. To better understand and explain it, dedicated studies were performed in TC2 using protection heaters

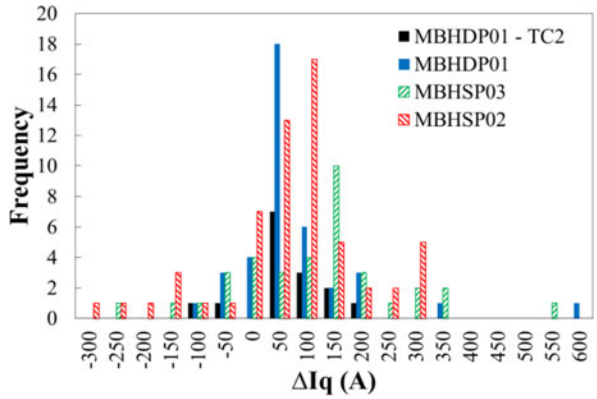

Fig. 7. Quench current differentials (difference of quench currents in consecutive training quenches) binned in 50 A ranges.

(PH). For each of the four coils there are two heater strips in the high field and two strips in the low field outer coil surface blocks with widths 26.0 mm and 21.5 mm, respectively. The two strips on one side of the pole - transition, T, or non-transition, NT, regions – are connected in series and form a single heater. Thus there are eight heaters in MBHDP01 and they cover about 56% of the total outer coil surface. With the exception of the width, strip parameters are all the same −0.025 mm thick stainless steel, separated from the coil by a 0.127 mm thick Kapton layer of ground insulation and a 0.125 mm epoxy impregnated S2-glass wrap.

In TC2 all PH studies were performed with only one heater firing on a half of a coil and all others being off. The dump was significantly delayed (up to 1000 ms) to allow reading the voltage tap signals. All tests were performed at 50 W/cm^2 power density with one exception where the density was 88 W/cm^2. In most of the tests PH5T (coil 5, transition region) was fired and a couple of additional tests fired either PH5NT or PH10T heaters. Studies were done at various currents –5, 7, 9, and 10.2 kA.

Fig. 8 compares the heater delays (time between heater firing and quench start time) observed in single and twin-aperture models vs. magnet current. In the twin-aperture, the heater delay dependence on the current is closely exponential (linear on the semi-log plot) in the range explored. The effect of the heater discharge time constant is consistent with the one observed in single-aperture models. The trend of the curve, however, deviated from exponential and the delay time was shorter in the single-aperture MBHSP02. Those effects are consistent with lower thermal contact resistance between heaters and coils in MBHSP02 due to the higher azimuthal and radial coil pre-stress relative to MBHDP01.

Fig. 9 makes similar comparisons for the outer (OL) to inner (IL) layer propagation times. The dependencies across models are consistent for the OL-IL quench propagation.

Fig. 10 shows voltage signals in coils 5, 7 and 9 and the magnet current ramp rate due to the increase of coil normal resistance after the heater induced quench in coil 10. The observations point to near-simultaneous, within few ms, quenching in all the three coils after the quench detection in coil 10.

Fig. 11 presents the coil-to-coil quench propagation times and the magnet current ramp-down rate at quench vs. magnet current. As the figure shows, the delay in coils has exponential dependence on the magnet current and has very weak heater power density dependence. At lower currents quenches start

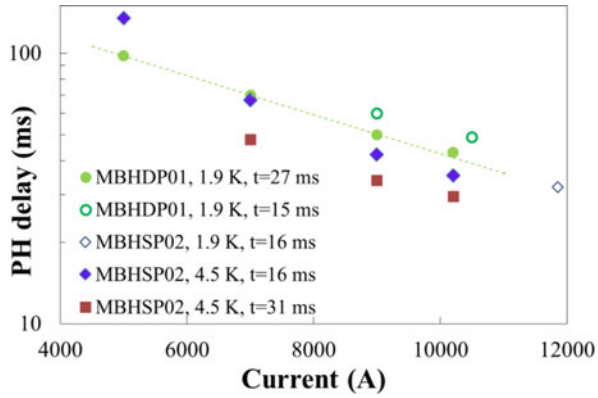

Fig. 8. Heater delay times vs magnet current at different temperatures and different decay constants. Temperatures do not affect delay times significantly and are given for completeness. MBHSP02 tests were with two-heater configuration (firing simultaneously); MBHDP01 at 15 ms decay constant were with four-heater configuration (TC1), and at 27 ms – single-heater configuration (TC2). In the twin-aperture model all times refer to coil 5.

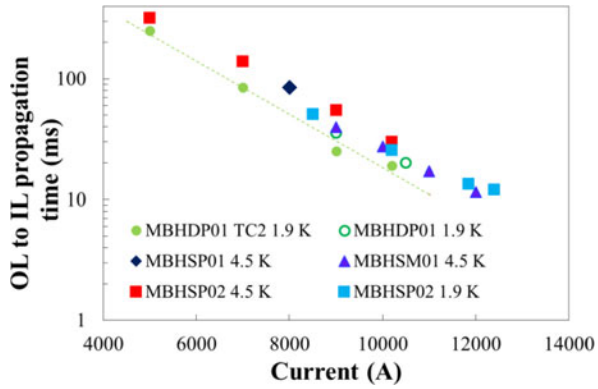

Fig. 9. Layer-to-layer quench propagation times. Tests were at power density of 50–56 W/cm^2 and 15–16 ms time constant except MBHDP01 TC2 which had 27 ms time constant.

to develop at lower ramp-down rates but take more time to start. The first segments to quench in all the coils are the same segments quenching during training. Quenches are observed in many other mostly inner layer segments within short intervals inconsistent with regular longitudinal (normal zone evolution) propagation. The primary hypothesis is that those quenches are caused by quench-back (AC loss induced quenches), although no quench-back was observed in the 11 T dipole mirror magnet MBHSM01 at higher dI/dt [6]. This discrepancy is being investigated.

V. Magnetic Measurements

The magnetic measurements were performed at 1.9 K using 130 mm 16-layer probe based on the Printed Circuit Board (PCB) technology [9]. The probe rotation speed was 1 Hz and the reference radius R_{ref} for the harmonic coefficients was 17 mm. The details of field quality measurements in MBHDP01 are reported in [10]. The measurement data were compared with 3D calculations of geometrical harmonics and iron saturation effects in the twin-aperture dipole model, as well as with magnetic measurements in single-aperture models [11], [12]. It was already shown [6], [13] that the large coil magnetization effect, seen in TF and b_3, is in good agreement with the calculations

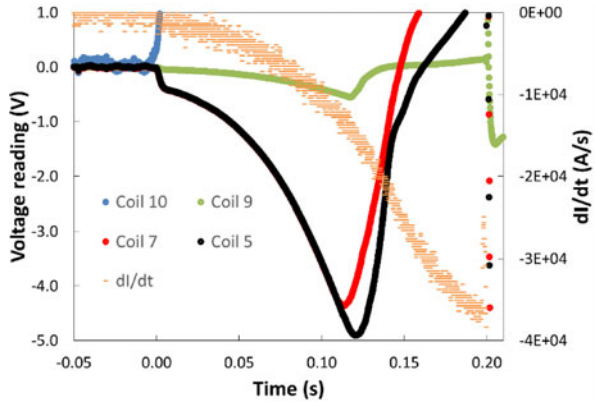

Fig. 10. Voltage signals in segments quenching first in a given coil. In this example the NT heater in coil 10 was firing and dump delay was 200 ms. The lengths and gains of the quenching segments differ but the increase in voltage indicates quenches occur at around +120 ms. The magnet current ramp-down rate is also given (secondary Y-axis). The magnet current was initially ramped to 9 kA.

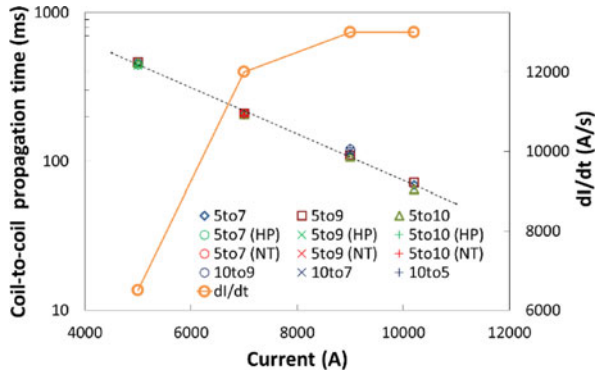

Fig. 11. Coil-to-coil quench propagation times. The first column is propagation in the same aperture, the next two – propagation to coils in the other aperture; the first row is the main result – power density of 50 W/cm^2 in a single heater in coil 5 (transition side); single tests were performed with higher power density ("HP", 88 W/cm^2), non-transition side heater ("NT") and heater firing in coil 10 (last row) instead of coil 5. An average dI/dt at the time of quench is also provided (secondary Y axis).

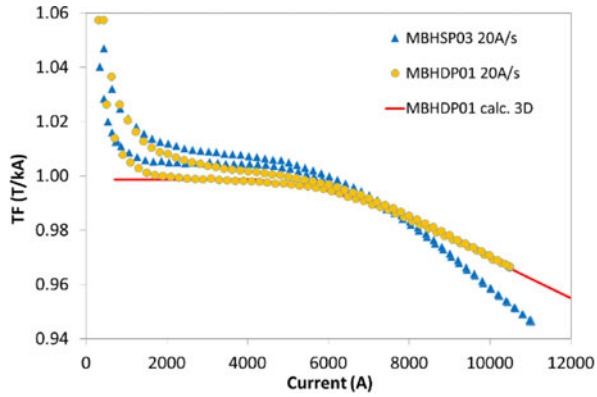

Fig. 12. Measured TF vs. current in single and twin-aperture models and 3D model calculations for the latter.

except for the coil re-magnetization part at low field which needs to be better understood [14].

Fig. 12 shows TF for MBHSP03 and MBHDP01. Figs. 13 and 14, respectively, present the b_2 and b_3 evolution vs. magnet current at a current ramp rate of 20 A/s. With respect to the single-aperture model, the twin-aperture dipole has slightly smaller

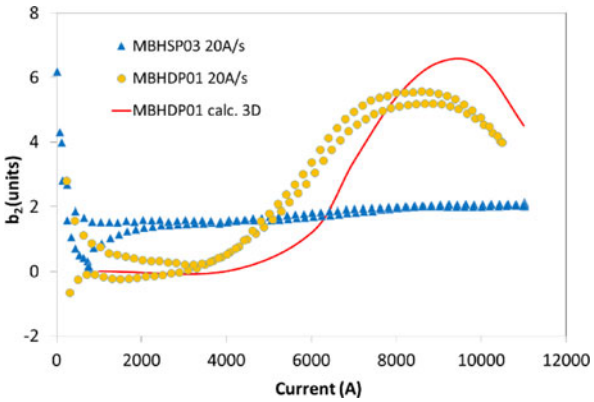

Fig. 13. Normal quadrupole b_2 vs. current in single and twin-aperture models.

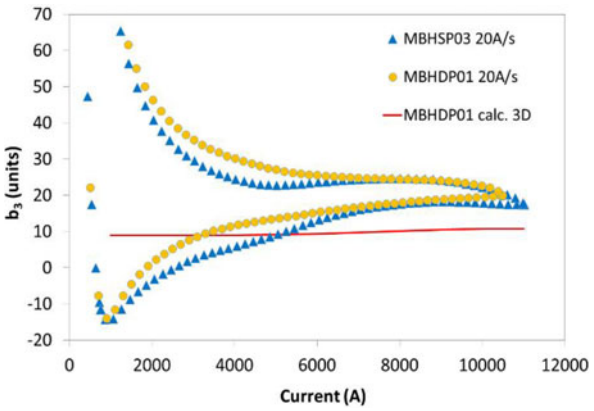

Fig. 14. Normal sextupole b_3 vs current in single and twin aperture models.

TABLE I
FIELD HARMONICS AT I = 3.5 KA

n	MBHSP02		MBHSP03		MBHDP01	
	a_n	b_n	a_n	b_n	a_n	b_n
2	0.1	−4.9	−4.6	1.4	−3.5	0.6
3	−1.4	8.4	2.0	16.1	0.4	20.9
4	0.2	−0.2	−0.1	0.1	0.3	0.3
5	0.2	1.0	−0.1	0.8	−0.5	−0.2
6	0.0	−0.2	−0.3	−0.2	−0.1	0.4
7	−0.1	0.0	0.0	0.3	−0.5	−0.2
8	0.0	0.0	0.1	0.0	0.1	0.2
9	0.1	0.2	0.2	1.3	0.5	1.1

iron saturation in TF and b_3 whereas b_2 is significantly affected due to the aperture cross talk. The small persistent current effect, seen in b_2 at low currents, is likely due to the asymmetry of magnet geometry and variations of coil magnetization.

Table I presents the geometrical harmonics at a magnet current of 3.5 kA for the single and twin-aperture models. The resolution of the measurements is better than 0.5 units. The higher order harmonics ($n > 3$) are small and only b_9 exceeds the resolution limit, similar to the single-aperture model with the same coils. On the other hand, different shimming between all models, used to achieve the target pre-stress levels, gives rise to sizable differences in the lower order harmonics.

VI. CONCLUSION

The FNAL 1 m long twin-aperture 11 T Nb_3 Sn dipole model MBHDP01 was re-tested in TC2 and its field parameters were measured. The magnet showed some re-training in TC2 which was rather slow. The quench performance at $T < 3$ K was slightly degraded, perhaps, by the presence of the "warm finger" used for the magnetic measurements. The magnet did not reach the same level of field in TC2. At higher temperatures the performance in the two thermal cycles was similar.

Near-simultaneous quench propagation between coils, including aperture-to-aperture, was observed with delay times depending exponentially on the magnet current. This effect may play an important role in LHC strategies for quench protection of Nb_3 Sn magnets. Heater delay times and propagation within the coil confirmed dependencies observed in single-aperture models but also revealed some deviations related to different pre-stress levels in single-aperture and twin-aperture models.

Finally, the iron saturation effects in the twin aperture model were smaller in TF and b_3 than in single aperture magnets but, as expected, significantly impacted the gradient field component b_2. The results for other harmonics are overall little changed with respect to single aperture models including geometrical harmonics and the persistent current effects.

ACKNOWLEDGMENT

The authors thank the staff of FNAL Technical Division for contributions to magnet design, fabrication, and test.

REFERENCES

[1] A. V. Zlobin *et al.*, "Development of Nb_3 Sn 11 T single-aperture demonstrator dipole for LHC upgrades," in *Proc. 2011 Particle Accelerator Conf.*, New York City, 2011, pp. 1460–1462.

[2] F. Savary *et al.*, "The 11 T dipole for HL-LHC: Status and plan," *IEEE Trans. Appl. Supercond.*, vol. 26, no. 4, Jun. 2016, Art. no. 4005305.

[3] A. V. Zlobin *et al.*, "Quench performance of the first twin-aperture 11 T dipole for the LHC upgrades," in *Proc. 6th Int. Particle Accelerator Conf.*, Richmond, VA, May 2015, pp. 3361–3364.

[4] A. V. Zlobin *et al.*, "Design and fabrication of a single-aperture 11T Nb_3 Sn dipole model for LHC upgrades," *IEEE Trans.Appl. Supercond.*, vol. 22, no. 3, Jun. 2012, Art. no. 4001705.

[5] M. Karppinen *et al.*, "Design of 11 T twin-aperture Nb_3 Sn dipole demonstrator magnet for LHC upgrades," *IEEE Trans. Appl. Supercond.*, vol. 22, no. 3, Jun. 2012, Art. no. 4901504.

[6] A. V. Zlobin *et al.*, "11 T Twin-aperture Nb_3 Sn dipole development for LHC upgrades," *IEEE Trans. Appl. Supercond.*, vol. 25, no. 3, Jun. 2015, Art. no. 4002209.

[7] G. Chlachidze *et al.*, "Experimental results and analysis from 11 T Nb_3 Sn DS dipole," FERMILAB-CONF-13-084-TD, and WAMSDO'2013 at CERN, Jan. 2013, CERN-2013-006, pp. 47–56.

[8] G. Chlachidze *et al.*, "Quench protection study of a single-aperture 11 T Nb_3 Sn demonstrator dipole for LHC upgrades," *IEEE Trans. Appl. Supercond.*, vol. 23, no. 3, Jun. 2013, Art. no. 4001205.

[9] J. DiMarco *et al.*, "Application of PCB and FDM technologies to magnetic measurement probe system development," *IEEE Trans. Appl. Supercond.*, vol. 23, no. 3, Jun. 2013, Art. no. 9000505.

[10] T. Strauss *et al.*, "Field quality measurements in the FNAL twin-aperture 11 T dipole for LHC upgrades," *NAPAC2016*, Chicago, Oct. 2016, FERMILAB-CONF-16-520-TD.

[11] N. Andreev *et al.*, "Field quality measurements in a single-aperture 11 304 T Nb_3 Sn demonstrator dipole for LHC upgrades," *IEEE Trans. Appl.* 305 Supercond., vol. 23, no. 3, Jun. 2013, Art. no. 4001804.

[12] G. Chlachidze *et al.*, "Field quality study of a 1-m long single-aperture 11 T Nb_3 Sn dipole model for LHC upgrades," *IEEE Trans. Appl. Supercond.*, vol. 24, no. 3, Jun. 2014, Art. no. 4000905.

[13] X. Wang *et al.*, "Validation of finite-element models of persistent-current effects in Nb_3 Sn accelerator magnets," *IEEE Trans. Appl. Supercond.*, vol. 25, no. 3, Jun. 2015, Art. no. 4003006.

[14] S. Izquierdo Bermudez *et al.*, "Persistent-current magnetization effects in high-field superconducting accelerator magnets," *IEEE Trans. Appl. Supercond.*, vol. 26, no. 4, Jun. 2016, Art. no. 4003905.